Resistor Current Noise Measurements

Frank Seifert (Frank.Seifert@aei.mpg.de)

April 14, 2009

Introduction

Excess low-frequency fluctuations are observed in many devices and materials [8, 22, 23] that carry a current. Because most materials and devices usually show a very low noise-level, the noise is hard to measure. Several different methods of measuring the excess noise in conducting materials have been discussed in literature [5]. Some techniques have in common that they focus on the phase sensitive readout of a standard, center-tapped Wheatstone bridge excited by one or more alternating currents. These include, amongst others the double frequency ac method [20], the 0°/90° subtraction method [18] and the 45° cross correlation technique [15, 16, 24, 25]. The advantage of these techniques is the separation or elimination of background noise (e.g. Johnson noise) from the excess noise to be measured. On the other hand, with low-noise amplifiers available today, the simple DC-measurement technique is also very powerful [1, 10].

There are several commonly used types of resistors: carbon, thin film, thick film, metal foil or wirewound. Each type has specific characteristics suitable for different applications with varying requirements. Thick-film resistors are made of a mixture of conductive particles (metallic grains) with a glassy binder and an organic fluid. This "ink" is printed on a ceramic substrate and heated in an oven. During this firing process the conductive particles within the glassy matrix are fused to the substrate and form the resistor. Thin film resistors are fabricated by sputtering a metal or alloy on an isolating substrate. Wirewound or foil-resistors are made from foils and wires of different metal alloys attached to an isolating substrate. All of them have in common that the total noise can be divided into thermal noise and excess noise. Excess current noise is the bunching and releasing of electrons associated with current flow, e.g. due to fluctuating conductivity based on imperfect contacts within the resistive material. The amount of current-noise depends largely on the resistor technology employed.

Current noise in materials is directly proportional to the current flowing through the device. The noise power density varies with the reciprocal of the frequency ($1/f$), rounding off at the point where it equals thermal noise. Current-noise of resistors is measurable and is expressed as a function of the voltage drop across a resistor. The amount of noise is expressed as a resistor-noise quality index. This index, the "microvolts-per-volt" index, is an expression for the rms noise voltage, in microvolts,

per volt of applied DC voltage, in volts, transmitted in a single frequency decade [3]. The noise index NI is expressed in decibels, and the equation converting µV/V to dB is

$$NI = 20 \log_{10} \left(\frac{v_{\mathrm{rms}}}{V_{\mathrm{DC}}} \right) \quad \text{[dB] in a decade} \tag{1}$$

with v_{rms} the root mean square noise voltage (in microvolts) and V_{DC} the voltage drop across the resistor. Therefore a noise index of $0\,\mathrm{dB}$ equates to $1\,\mathrm{µV/V}$. It should be noted that the same amount of noise power is transmitted in a frequency decade regardless of the absolute frequency, if the noise has a true $1/f$ spectrum. In general, the mean-square noise voltage is given by

$$\overline{v^2} = \int_{f_1}^{f_2} S(f) df = \int_{f_1}^{f_2} \frac{\overline{e^2(f)}}{\Delta f} df \tag{2}$$

where $S(f)$ is the PSD of the measured resistor current-noise in the frequency band f_1 to f_2 and $\frac{\overline{e^2(f)}}{\Delta f}$ is the mean-square noise voltage spectral density at frequency f. The power spectral density of current noise is commonly assumed to be proportional to $1/f$. Then the product of the PSD and frequency is constant and Equation 2 can be rewritten as

$$\overline{v^2} = \frac{\overline{e^2(f)}}{\Delta f} f \int_{f_1}^{f_2} \frac{df}{f} \tag{3}$$

$$= \frac{\overline{e^2(f)}}{\Delta f} f \ln \frac{f_2}{f_1} \tag{4}$$

$$= \frac{\overline{e^2(f)}}{\Delta f} f \ln 10 \qquad \text{for one decade} \, (f_2 = 10 f_1) \tag{5}$$

The root mean square noise voltage can now be expressed using the noise index as

$$v_{\mathrm{rms}} = \sqrt{\overline{v^2}} = V_{\mathrm{DC}} \cdot 10^{NI/20} \sqrt{\log_{10} \frac{f_2}{f_1}} \qquad [\mu V_{\mathrm{rms}}] \text{ in frequency band } f_1 \text{ to } f_2 \tag{6}$$

$$= V_{DC} \cdot 10^{NI/20} \qquad [\mu V_{\mathrm{rms}}] \text{ in one decade} \tag{7}$$

Based on the IEC recommendation [9] and MIL-STD-202, Method 308 [21] for measuring the current noise generated in fixed resistors, a low-noise measurement setup for excess noise measurements of several commercial available resistors was built and a large quantity of resistors was characterized.

Experimental Setup

Although the DC-measurement technique has several limitations, it has been used to measure the excess noise of commercial available resistors used in our institute.

The disadvantage of this technique is, that the overall performance is limited by the background noise (Johnson noise of the resistors and amplifier input noise). Nevertheless this technique is sufficient, because the main interest for this thesis was to find the excess noise which limits the overall performance of the power stabilization setup. The measurement setup is illustrated in Figure 1.
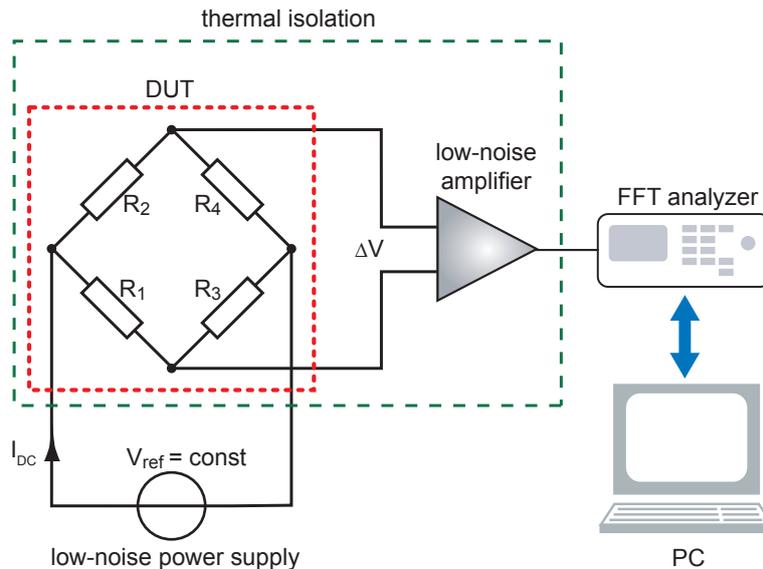

Figure 1: Resistor current noise measurement setup using a full Wheatstone bridge configuration.

The tested resistors (DUT) are connected in a voltage-driven full Wheatstone bridge configuration. Traditionally, the voltage-driven Wheatstone bridge configuration is used for precise measurement of small resistance changes, but can be also used for resistor current noise measurements. The excitation voltage V_{ref} is applied across one diagonal of the bridge and a constant current $I_{\mathrm{DC}}/2$ flows through all four resistors of the bridge. The output voltage of the bridge ΔV is measured differentially across the other diagonal.

For resistor current noise measurements, the bridge current I_{DC} through the resistors under test was supplied by an adjustable, low-noise, high current voltage source. In order to avoid disturbances coming from the power supply and other common mode interference, the use of differential configurations is mandatory. The noise voltage across the bridge was amplified by an ultra low-noise differential amplifier optimized for the impedance of the DUT. The amplifier output is fed into an FFT analyzer, which was remotely controlled by a personal computer running a LabVIEW® program for automated noise measurements. To obtain a high resolution spectrum over the entire frequency range accessible by the analyzer, the noise measurements were repeated a few times with different parameters in order to combine different bandwidth-frequency resolutions. The entire bridge and the

differential amplifier are mounted in a aluminum box for thermal shielding against air currents and electromagnetic interferences and was supplied using batteries to reduce disturbances from line harmonics.

The nominal values of the four resistors of the full bridge R_1 to R_4 are chosen to be equal (R_0). Thus the impedance of the bridge seen by the amplifier is R_0. By means of careful selection of modern integrated circuits, the equivalent input noise of a voltage amplifier can be reduced to a minimum, close to the thermal noise limit of the setup. For a resistance R_0 up to $1\,\mathrm{k\Omega}$, a low-noise instrumentation amplifier INA103 (Texas Instruments) with a gain $G = 60\,\mathrm{dB}$ was used, for higher values of R_0 the AD620 (Analog Devices) with a gain $G = 40\,\mathrm{dB}$ was used. The performance characteristics of the amplifiers are listed in Table 1.

	INA103, 60 dB gain	AD620, 40dB gain
input current-noise density i_n	$0.7\,\mathrm{pA}/\sqrt{\mathrm{Hz}}$	$6.3\,\mathrm{fA}/\sqrt{\mathrm{Hz}}$
noise corner frequency for i_n	$223\,\mathrm{Hz}$	$20\,\mathrm{Hz}$
input voltage noise density v_n	$1.15\,\mathrm{nV}/\sqrt{\mathrm{Hz}}$	$9.9\,\mathrm{nV}/\sqrt{\mathrm{Hz}}$
noise corner frequency for v_n	$6\,\mathrm{Hz}$	$4.5\,\mathrm{Hz}$
bandwidth	$100\,\mathrm{kHz}$	$65\,\mathrm{kHz}$

Table 1: Measured differential amplifier data for the resistor current-noise measurement setup.

In order to evaluate the influence of the bridge excitation voltage to the noise performance on the noise measurement setup, the common-mode rejection ratio (CMRR) of the full bridge has to be estimated. The largest differential signal ΔV and hence imbalance of the bridge is achieved when opposite resistors in the bridge change resistance as shown by $\pm \Delta R$

$$R_1 \quad = \quad R_4 = R_0 \pm \Delta R \tag{8}$$
$$R_2 \quad = \quad R_3 = R_0 \mp \Delta R \tag{9}$$

The differential voltage ΔV across the bridge is given by

$$\Delta V = \pm \frac{\Delta R}{R_0} \cdot V_\mathrm{ref} \tag{10}$$

Since the bridge sensitivity $\Delta V / (\Delta R / R_0)$ is proportional to V_ref, also the noise signal obtained from the bridge is sensitive to the noise of the excitation voltage. Thus, for the current-noise measurement, the resistors are matched in a way that the differential voltage across the bridge is as small as possible and hence the voltage noise of the excitation voltage is suppressed by a large factor.

The maximum output for the differential amplifier is $\approx 10\,\mathrm{V}$. Therefore, for a minimum gain of $40\,\mathrm{dB}$, the maximum input voltage of the amplifier can be $100\,\mathrm{mV}$. Thus, as a worst case for a $10\,\mathrm{V}$ bridge supply, the mismatch of resistance can be 1%, which corresponds to a common-mode reduction for the excitation noise of $40\,\mathrm{dB}$.

For higher gains of the amplifier the bridge mismatch allowed that does not saturate the amplifier is even lower and therefore the common-mode reduction even higher.

In order to estimate the limitations due to the bridge excitation voltage, the output voltage noise of the voltage source for several DC output levels was measured. The noise induced by the voltage source must be well below the thermal noise of the bridge impedance. As derived above, the CMRR of the bridge for the excitation noise equals the gain as a minimum. Thus the influence of a noisy excitation voltage on the measurement can be estimated. The noise projection of the excitation for different voltage levels of V_{ref} $(1, 2, 5, 10\,\mathrm{V})$ assuming a minimum CMRR of $40\,\mathrm{dB}$ of the balanced bridge is shown in Figure 2.
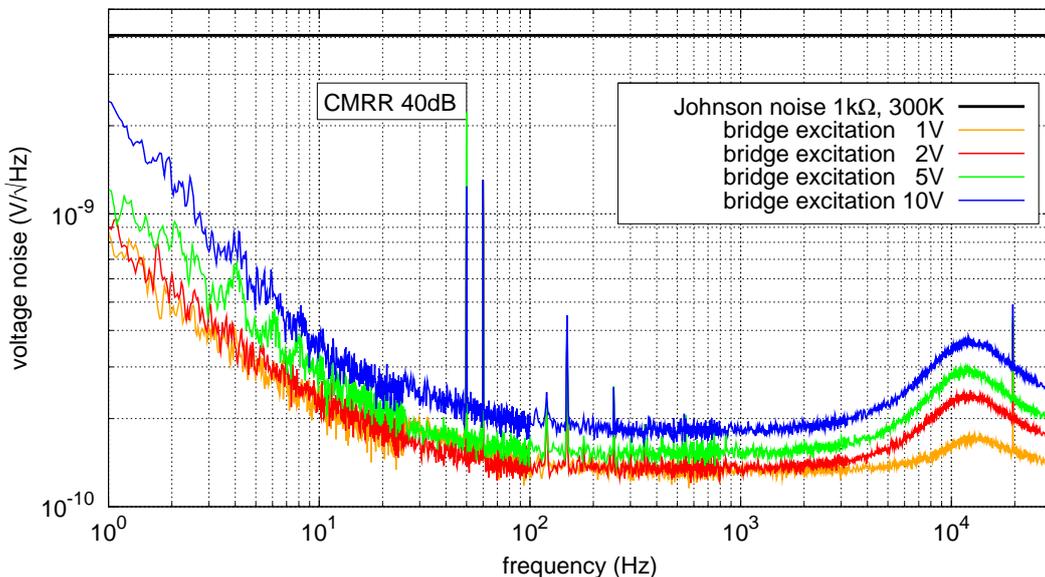
Figure 2: Noise projection of the high current voltage source for different voltage levels assuming a minimum CMRR of $40\,\mathrm{dB}$ of the balanced bridge.

Using the low-noise power supply, the noise reduction is sufficient so as not be the limiting factor. With the lowest gain of $40\,\mathrm{dB}$, the noise level is comfortably below the minimum thermal noise limit of the bridge ($1\,\mathrm{k\Omega}$ impedance). For resistor values below $1\,\mathrm{k\Omega}$, the gain was $60\,\mathrm{dB}$ and so the noise of the excitation voltage at least one order of magnitude below the plotted spectra. The intended minimum resistance value to be measured is $100\,\Omega$ $(\approx 1.3\,\mathrm{nV}/\sqrt{\mathrm{Hz}}$ thermal noise), which is large compared to the maximum excitation noise expected for $60\,\mathrm{dB}$ of gain. The electronic schematic is shown in Figure 3.

In practice, the overall sensitivity is limited by the thermal noise of the bridge itself and the differential amplifier input voltage and current-noise, especially at low frequencies. Since the input voltage and current noise spectral densities of the differential amplifiers can be assumed to be constant, these noise sources can be characterized carefully and subtracted from the noise measurements of the DUT.
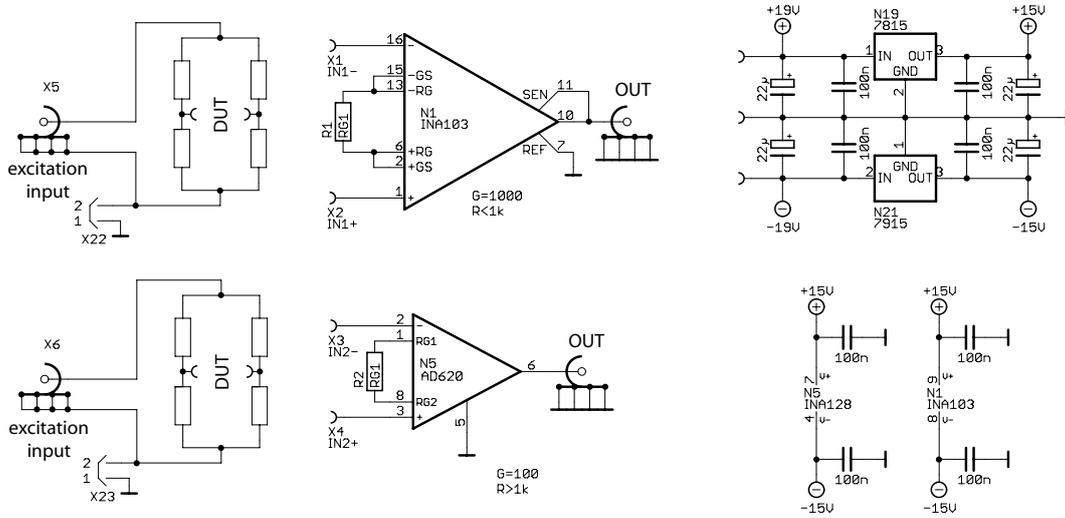
Figure 3: Resistor current noise measurement setup - electronic schematic

The input noise of the two differential amplifiers used was measured for several different bridge impedances distributed over the entire measurement range. For low impedances the total noise is dominated by the input voltage noise of the amplifier, for high impedances by the current noise. From the data obtained, the noise contribution of the voltage and current noise of the input was calculated and a model for each amplifier was generated. Later, these models were used to subtract the amplifier input noise for the impedance of the DUT. This enables measurements down to the thermal noise equivalent to the input noise of the amplifiers or even below.

As the current noise of resistors scales with the voltage drop across it, the bridge supply was chosen to be 10 V for all noise measurements. The voltage across one resistor is then half the excitation voltage. Since the current noise of the resistors is uncorrelated, the noise contribution of all four resistors of the bridge sum up to a factor of two. Thus the measured noise of a complete bridge can be interpreted as an estimate for the noise of one of its resistors driven by the full 10 V. The noise index and thus the product quality is estimated from measurements on a group of nominally "identical" resistors. All resistors are tested at the same excitation voltage, $V_{ref} = 10$ V. Hence the differences in the measured noise can be attributed to excess current noise of the tested devices.

Results

As reported in the literature, the current noise of resistors is linear with the voltage drop across it. An experiment for some typical resistors used in our institute was conducted to evaluate the amount of current noise as a function of applied excitation voltage. A typical plot of noise spectra for several voltage drops from 0 V to 10 V is shown in Figure 4.
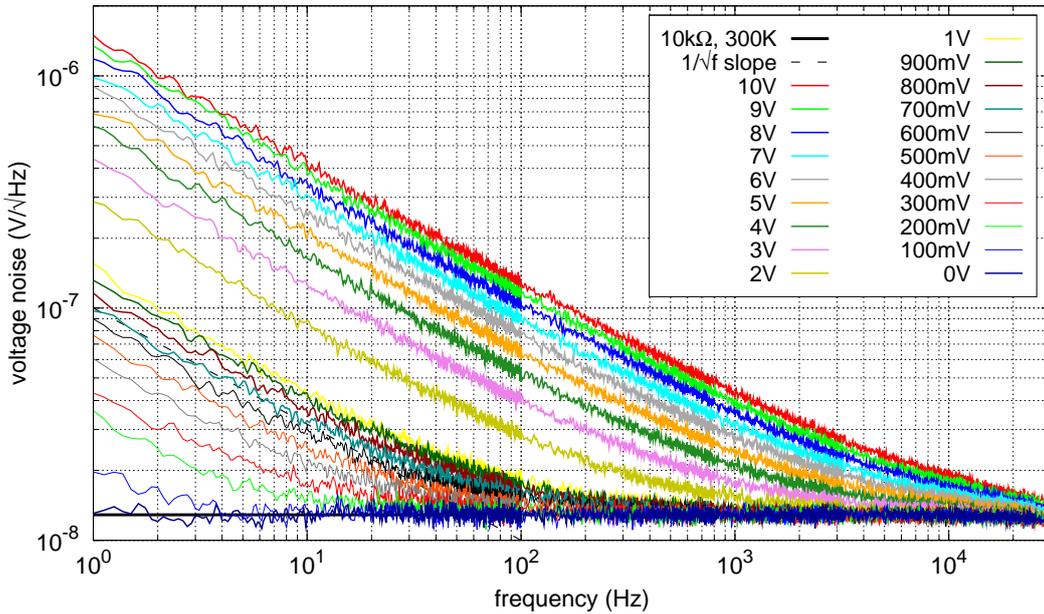
Figure 4: Resistor current noise spectra for different excitation voltages (in units of the corresponding voltage drop fluctuations).

As expected, the noise level increases with rising voltage drop at low frequencies. In order to demonstrate the linearity, the noise level of each graph at Fourier frequencies 1 Hz, 10 Hz and 100 Hz has been taken and plotted against the voltage drop. The result is shown in Figure 5. The measurement points obtained from the individual spectra were fitted using a linear regression. The increasing noise spectra is linear over the entire range from 0 V to 10 V of the excitation voltage, which is in agreement with the literature.

Tests on a large number of different manufacturers' products were performed. All measurements were performed at room temperature within a frequency range of between 1 Hz and 30 kHz for three groups of resistors having nominal values of $100\,\Omega$, $1\,k\Omega$ and $10\,k\Omega$. Each group consisted of 4 identical samples (one full bridge). Higher and lower values are often not needed and it is expected that devices with higher resistivity values of the same type of resistor have even higher excess noise. This expectation is supported by datasheets where the manufacturers give typical values for the noise index of their products.

In the following all results for values of $100\,\Omega$, $1\,k\Omega$ and $10\,k\Omega$ are summarized. A total number of 60 different types of resistors with a nominal value of $100\,\Omega$ were characterized. They were split into four different categories: surface-mount devices (SMD) up to a maximum power dissipation of 1 W, leaded parts up to 1 W, power resistors from 1 W to 5 W and high power resistors with more than 5 W maximum power rating. The results are summarized in Figures 6 to 9. For a nominal values of $1\,k\Omega$ and $10\,k\Omega$ less different types were characterized. These results are summarized
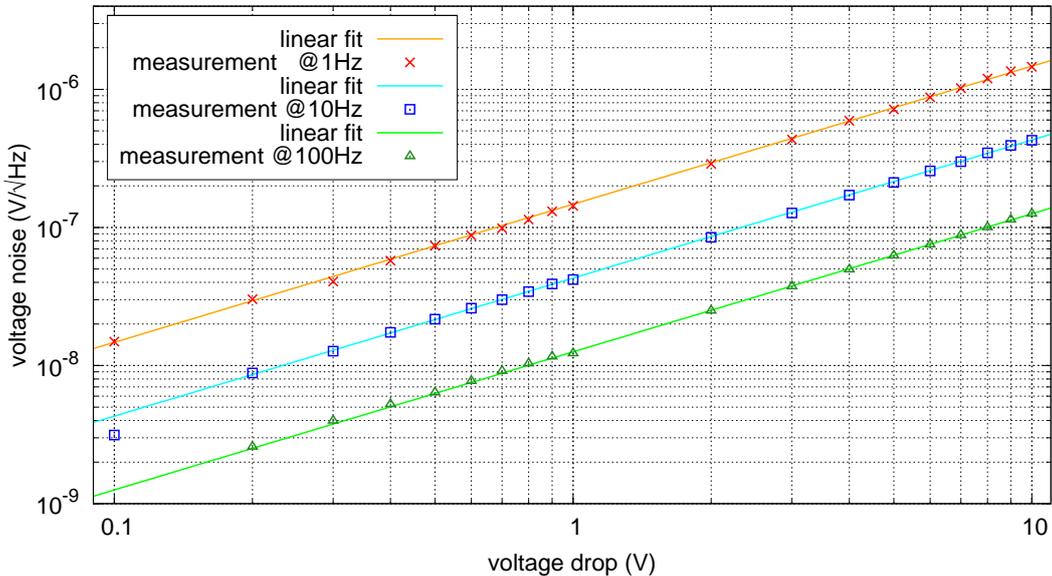
Figure 5: Resistor current noise as a function of voltage drop (in units of the corresponding voltage drop fluctuations).

in Figures 10 and 11. In some of the tested devices popcorn noise was observed. As an example the measured noise in a thick film resistor using an oscilloscope is shown in Figure 12.

This study has pointed out that excess noise can be observed in all kind of resistors tested and used in our designs. The observed level varies over almost three orders of magnitude and depends on several parameters like type, size, wattage, process, manufacturer, etc. Because of this it is very hard to find the ideal resistor for every day usage in the lab. For comparison, the calculated noise spectra for resistors having a noise index of -20 dB, -40 dB and -60 dB are plotted as well.

For frequencies above 1 Hz, the very expensive ultra high precision Bulk Metal® Z-Foil and classical wirewound resistors appear to have very little or no excess noise. Wirewound resistors however, do have inductance that may affect the circuit operation. Metal film or thin film resistors have little excess noise in these tests and thick film resistors show large excess noise [26, 27]. It could be observed that the noise decreases with increasing mechanical size or volume of the same type of resistor, which is in agreement with experiments reported in the literature [4, 12, 13, 17]. For the same resistance value and current, a higher power resistor of the same style will generate less noise. Furthermore, the excess noise has a linear voltage dependence as reported in the literature [7]. The temperature dependence of the low-frequency noise has not been measured, but it can be found in the literature that the $1/f$-noise in resistors can be temperature dependent [2, 6, 14]. These papers suggest that a change in temperature changes the distribution of relaxation times of the noise process due to changes of the microstructure. This is only important for large changes
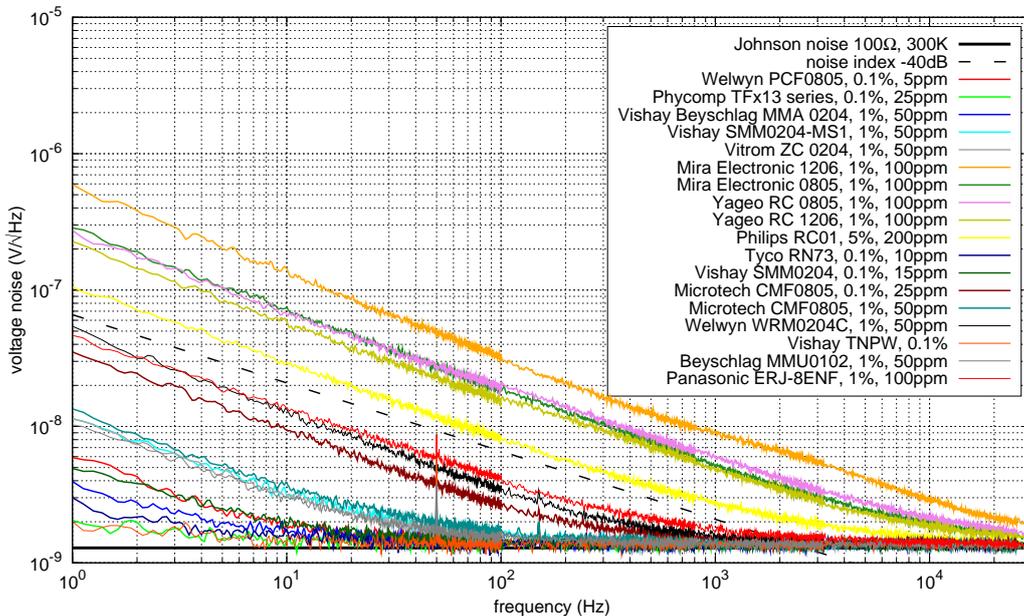
Figure 6: Current noise of surface-mount devices (SMD) with $100\,\Omega$ up to a maximum power dissipation of $1\,\mathrm{W}$.

in temperature, not for operating conditions around room temperature.

The data presented in this work offers a background for evaluating noise in electronic designs which to date is not implemented in standard simulation software. Even though the noise level largely depends on the voltage drop, an upper limit can be set by assuming an potential difference equal to the supply voltage. Furthermore sample-to-sample variations have to be taken into account. Hence a pre-selection of critical components is suggested before their use in a circuit. The results given here are well suited for an estimation of the amount of excess noise for existing electronics, which can then be easily optimized.

A more detailed noise study for lower frequencies will be performed in the near future to get similar data for devices used in the LISA and LISA-Pathfinder electronics. Because measurements at lower frequencies are very sensitive to thermal disturbances, these measurements will be performed with one of the phase sensitive readout schemes. Furthermore only a few publications on low-frequency noise in capacitors are available [11, 19]. Hence a careful noise characterization of capacitors should be considered as well.
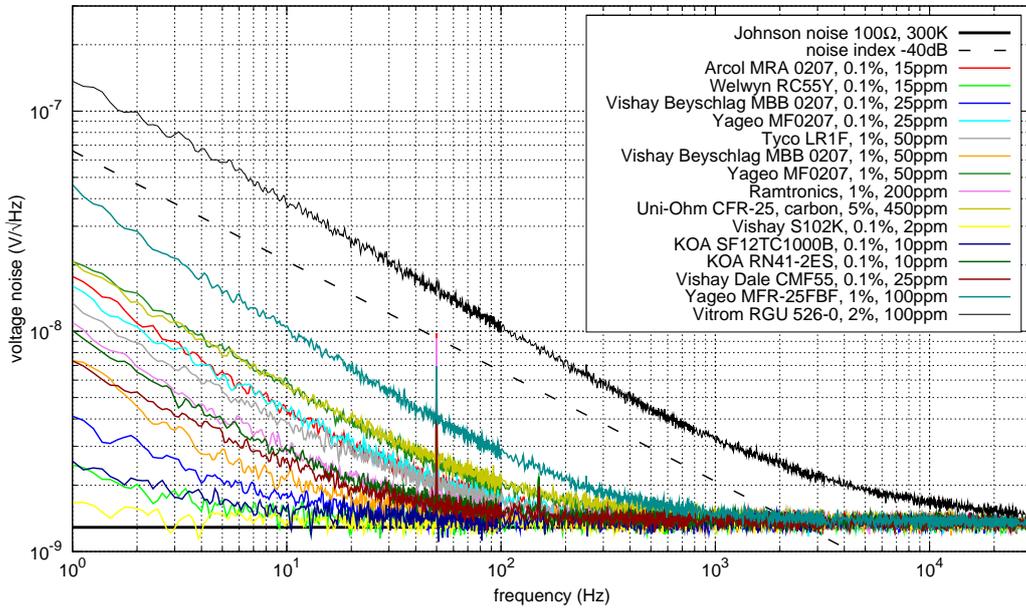
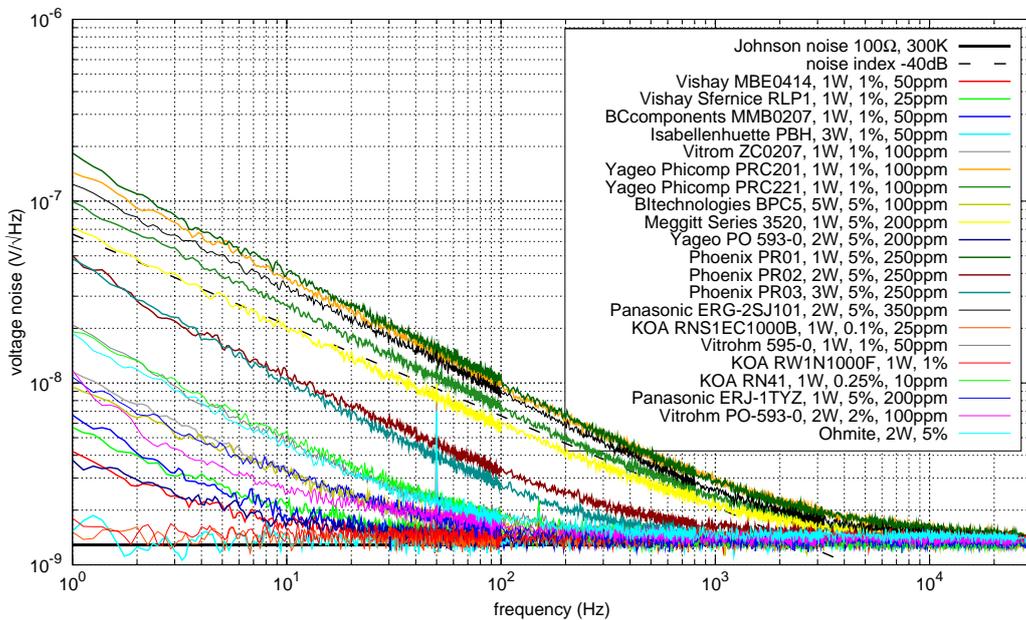**Figure 7:** Current noise of leaded resistors with $100\,\Omega$ up to a power rating of $1\,W$.

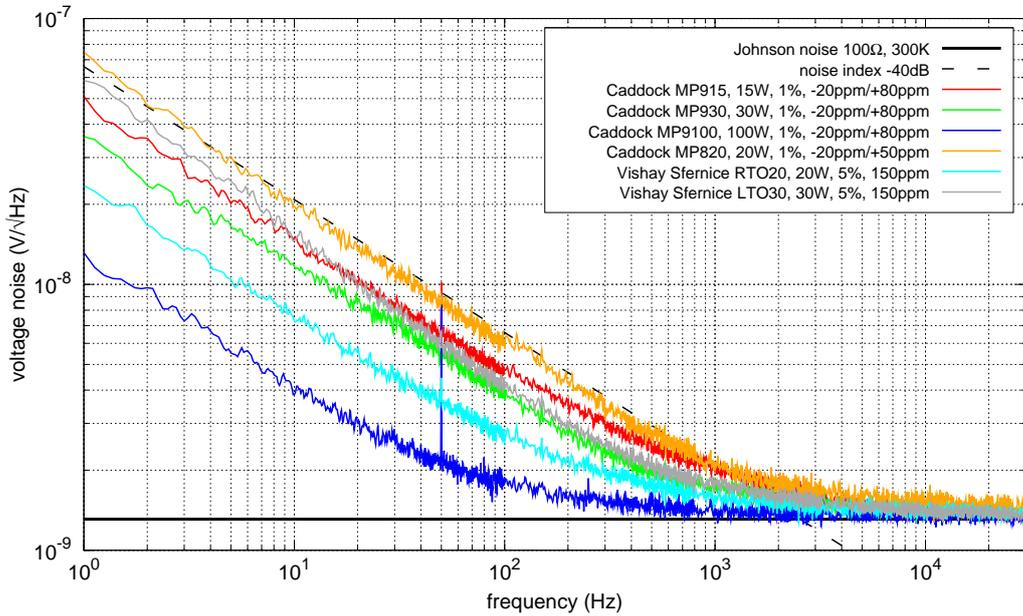**Figure 8:** Current noise of power resistors with $100\,\Omega$ from $1\,W$ to $5\,W$.

Figure 9: Current noise of high power resistors with $100\,\Omega$ and more than $5\,\mathrm{W}$ maximum power rating.
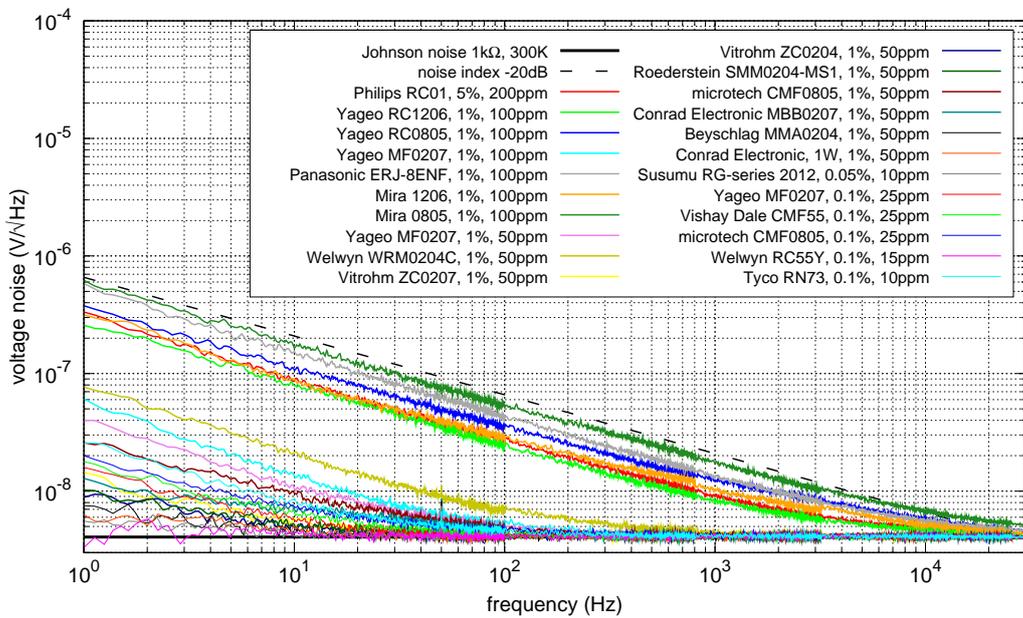

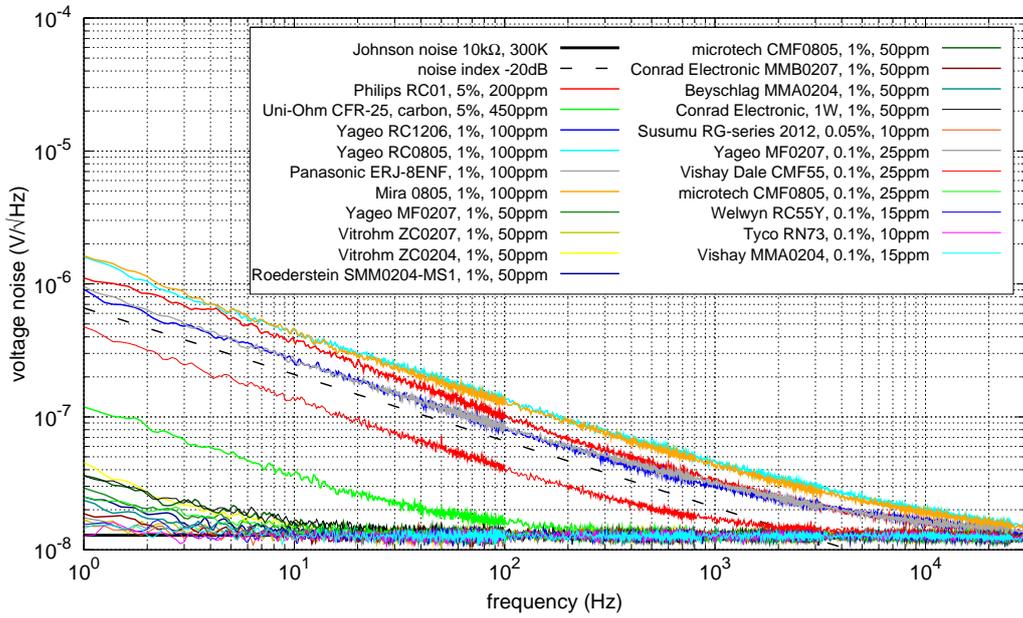**Figure 10:** Current noise of resistors with a nominal value of $1\,\mathrm{k}\Omega$.

Figure 11: Current noise of resistors with a nominal value of $10\,\mathrm{k\Omega}$.
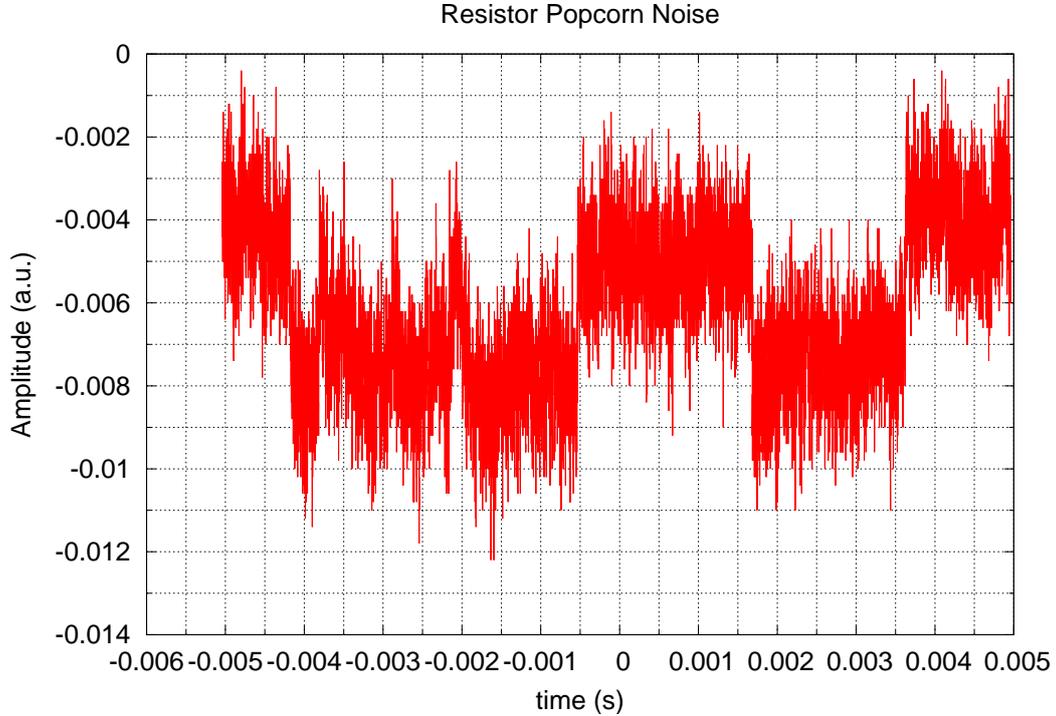

Figure 12: Popcorn noise observed in a thick film resistor.

References

[1] A. Blaum, O. Pilloud, G. Scalea, J. Victory, and F. Sischka. A new robust on-wafer $1/f$ noise measurement and characterization system. *Microelectronic Test Structures, 2001. ICMTS 2001. Proceedings of the 2001 International Conference on*, pages 125–130, 2001.

[2] T. M. Chen, S. F. Su, and D. Smith. $1/f$ Noise in Ru-Based Thick-Film Resistors. *Solid-State Electronics*, 25(8):821–827, 1982.

[3] Jr. Conrad, G., N. Newman, and A. Stansbury. A Recommended Standard Resistor-Noise Test System. *Component Parts, IRE Transactions on*, 7(3):71–88, September 1960.

[4] G. De Mey. Comments on "An exact formula for the effects of resistor geometry on current noise". *Electron Devices, IEEE Transactions on*, 34(8):1838–1838, August 1987.

[5] S. DEMOLDER, M. VANDENDRIESSCHE, and A. VANCALSTER. The measuring of $1/f$ noise of thick and thin-film resistors. *Journal Of Physics E-Scientific Instruments*, 13(12):1323–1327, 1980.

[6] D.M. Fleetwood, T. Postel, and N. Giordano. Temperature dependence of the $1/f$ noise of carbon resistors. *Journal of Applied Physics*, 56(11):3256–3260, 1984.

[7] R.J. Hawkins and G.G. Bloodworth. Measurements of low-frequency noise in thick film resistors. *Thin Solid Films*, 8(3):193–197, September 1971.

[8] F.N. Hooge. $1/f$ noise sources. *Electron Devices, IEEE Transactions on*, 41(11):1926–1935, November 1994.

[9] IEC. Method of measurement of current noise generated in fixed resistors, 1965.

[10] A. Kerlain and V. Mosser. Robust, versatile, direct low-frequency noise characterization method for material/process quality control using cross-shaped 4-terminal devices. *Microelectronics and Reliability*, 45(9-11):1327–1330, 2005.

[11] Alicja Konczakowska. $1/f$ noise of electrolytic capacitors as a reliability indicator. *Quality and Reliability Engineering International*, 14(2):83–85, 1998.

[12] D.P. Levinson and A.D. Snider. An exact formula for the effects of resistor geometry on current noise. *Electron Devices, IEEE Transactions on*, 33(1):58–60, January 1986.

[13] A. Masoero, B. Morten, M. Tamborin, and Prudenziati M. Excess noise in thick film resistors: Volume dependence. *Microelectronics International*, 12(3):5–8, 1995.

[14] A Masoero, A M Rietto, B Morten, and M Prudenziati. Excess noise and its temperature dependence in thick-film (cermet) resistors. *Journal of Physics D: Applied Physics*, 16(4):669–674, 1983.

[15] J. S. MOON, A. F. MOHAMEDULLA, and N. O. BIRGE. Digital measurement of resistance fluctuations. *Review Of Scientific Instruments*, 63(10):4327–4332, October 1992.

[16] A. RAAB, C. JUNG, and P. DULLENKOPF. Current noise of trimmed thick-film resistors: measurement and simulation. *Microelectronics International*, 15(1):15–22, 1998.

[17] D. Rocak, D. Belavic, M. Hrovat, J. Sikula, P. Koktavy, J. Pavelka, and V. Sedlakova. Low-frequency noise of thick-film resistors as quality and reliability indicator. *Microelectronics Reliability*, 41(4):531–542, April 2001.

[18] J. H. SCOFIELD. AC Method For Measuring Low-Frequency Resistance Fluctuation Spectra. *Review Of Scientific Instruments*, 58(6):985–993, June 1987.

[19] D.T. Smith. Low frequency noise in tantalum capacitors. *Active and Passive Electronic Components*, 12(4):215–221, 1987.

[20] H. STOLL. Analysis of resistance fluctuations independent of thermal voltage noise. *Applied Physics*, 22(2):185–187, 1980.

[21] U.S. Department of Defense. MIL-STD-202G, METHOD 308 - Current-Noise test for fixed resistors, November 1961.

[22] A. van der Ziel. Noise in solid-state devices and lasers. *Proceedings of the IEEE*, 58(8):1178–1206, August 1970.

[23] A. van der Ziel. Unified presentation of $1/f$ noise in electron devices: fundamental $1/f$ noise sources. *Proceedings of the IEEE*, 76(3):233–258, March 1988.

[24] Aldert van der Ziel. *Noise. Sources, characterization, measurement.* Prentice-Hall Information and System Sciences Series, Englewood Cliffs: Prentice-Hall, 1970, 1970.

[25] A. H. Verbruggen, H. Stoll, K. Heeck, and R. H. Koch. A novel technique for measuring resistance fluctuations independently of background-noise. *Applied Physics A-Materials Science & Processing*, 48(3):233–236, March 1989.

[26] Vishay. Audio noise reduction through the use of bulk metal foil resistors - "hear the difference". Technical report, Vishay, July 2005.

[27] Vishay. High-precision bulk metal foil resistors for military and aerospace applications. Technical report, Vishay, September 2005.